SINGLE MOLECULE TRACKING STUDIES OF SOLVENT-SWOLLEN MICRODOMAINS IN CYLINDER-FORMING POLYSTYRENE-POLY (ETHYLENE OXIDE) DIBLOCK COPOLYMER FILMS

by

DOL RAJ SAPKOTA

B.S., Tribhuvan University, 2003
M.S., Tribhuvan University, 2005

A THESIS

Submitted in partial fulfillment of the requirements for the degree

MASTER OF SCIENCE

Department of Chemistry
College of Arts and Sciences

KANSAS STATE UNIVERSITY
Manhattan, Kansas

2016

Approved by:

Major Professor
Takashi Ito

Copyright

Abstract

Solvent swelling of block copolymer microdomains plays an essential role in the improvement of microdomain alignment by solvent vapor annealing and in chemical separations using block copolymer monoliths. Here, investigation of the effects of solvent swelling on the molecular permeability and dimensions of cylindrical microdomains in polystyrene-*block*-poly(ethylene oxide) (PS-*b*-PEO) films is done by using single molecule tracking. These films are prepared by sandwiching benzene (with/without methanol) or THF (with/without methanol) solutions containing 5 nM sulforhodamine B (SRB) between two glass substrates. The PEO microdomains are aligned in the solution flow direction during the film preparation. The diffusional motions of individual SRB molecules are measured at different drying times to assess the microdomain radius and permeability. These parameters, on average, gradually decrease with an increase in drying time; however the trend differs slightly from one solvent system to another. A sharp decrease of microdomain radius is observed for benzene, benzene-methanol, THF and THF-methanol swollen films at initial drying condition (for example 2 days). In contrast, microdomain permeability does not decrease sharply; instead a gradual decreasing trend is seen for all solvent systems. In addition, mixing of a small amount of methanol (14% in PEO microdomains) either with benzene or with THF does not produce noticeable difference in the swelling of PEO microdoamins. Importantly, both benzene and THF offer similar microdomain swelling behavior at the same drying temperature, which is evident from the microdomain radius values, however THF shows comparatively larger microdomain permeability and better correlation between permeability and microdomain radius compared with benzene.

Table of Contents

List of Figures

Acknowledgements

I would like to thank my advisor Dr. Takashi Ito for guiding me throughout my graduate study. I imagined working and carrying out research in his guidance when I was in my home country. When I started my study and research, his constant support inspiration and encouragement was highly appreciable. He was always supportive throughout my pursuit of the Master's Degree, which enabled me to develop a better understanding of the study. I feel lucky for getting opportunity to work and learn under his supervision.

I would also like to thank Dr. Khanh-Hoa Tran-Ba for helping me from the beginning of my graduate study. He taught me both experimental and theoretical concepts of my research which was really helpful to collect and analyze data. Thanks to all the Ito's present group members (Govinda Ghimere, Herman Coceancigh, Zeinab Harandizadeh, Trevor Elwell-Cuddy and Roberto Espinosa) and past group members including Bipin Pandey who guided and encouraged me during my study in Kansas State University. Similarly, I would like to thanks Higgins group members. They were always sharing their research skills and were very helpful in lab.

I would also like to thank all of my committee members, Dr. Daniel Higgins, Dr. Stefan Bossmann. Also, I would like to thank Ron Jackson, Tobe Eggers, James Hodgson, Mary Dooley and others in the Kansas State University Chemistry Department who help me directly and indirectly to make my graduate study successful and memorable. Finally, I would like to show my appreciation for my family and friends for their constant love and support.

Dedication

This work is dedicated to my father Lila Ballav Sapkota, mother Sabitra Sapkota, wife Tika Kumari Luitel (Sapkota), my beautiful daughters Alisha Sapkota, Aayusha Sapkota and my country Nepal.

Chapter 1- Introduction

This thesis describes the swelling behavior of three different solvents including benzene, tetrahydrofuran and methanol on the cylindrical polyethylene oxide (PEO) microdomains of a polystyrene-block-poly(ethylene oxide) diblock copolymer (PS-*b*-PEO). Depending on the nature of solvent used, swelling of PEO microdomain is expected to vary.

In this chapter, first of all, the objectives and motivation for carrying out the studies in the PS-*b*-PEO will be explained. This will be followed by background/literature review section which gives a brief overview of cylindrical morphologies obtained by the self-assembly and microphase separation of block copolymers. Similarly, ways of making polymer films containing cylindrical microdomains, effects of various solvents on the formation of PEO microdomains/nanopores and characterization by single molecule tracking (SMT) method will be discussed.

1.1 Objectives and Motivation

Cylindrical microdomains fabricated from block copolymers are attracting significant interest because of their possibility in various applications. This thesis aims to explain solvent-swollen cylindrical PEO microdomains of PS-*b*-PEO and characterization by using single molecule tracking (SMT). Here, the way to fabricate cylindrical PEO microdomains and how a particular solvent behaves in the swelling of PEO microdomains will be explained. In order to study solvent-swollen PEO microdoamins, SMT is used which is very useful for getting nanoscale information of the individual PEO microdoamins. Through this study, microdomain dimensions and permeability at wet and dried conditions can be estimated for each solution composition which will help to explain the property of PS-*b*-PEO and in particular PEO microdomains. Another objective of this study is to correlate the diffusion coefficient and

microdomain radius in different solvent system. This correlation will help to understand whether larger diffusion coefficients coincide with larger radius or vice versa. This study on the PS-*b*-PEO is very important to explore their possible applications in chemical separation, sensing, nanomaterial synthesis, lithographic masks and more.

1.2 Background/Literature review

1.2.1 Cylindrical microdomains from block copolymers

Block copolymers (BCPs) are polymers consisting of two or more distinct homopolymer fragments connected by covalent bonds. BCPs have the ability to self-assemble into arrays of various well-defined structures such as spheres, cylinders, or lamellae depending upon the volume fraction and length of the individual polymer fragments.[1-4] In recent years, cylinder-forming block copolymers having characteristic dimensions are getting significant attention in the polymer research because of their possibilities in various applications including templates for nanomaterial synthesis, photolithographic masks, and membranes for chemical separations and sensing,[1-6]drug delivery,[8] and catalysis.[9] In order to explain the formation of cylindrical morphology from block copolymer melts, a phase diagram is necessary which is shown in Figure 1.1.[10]. This phase diagram uses two parameters f and χN to explain block copolymer morphology. The volume fraction of one block is represented by f which is present on the x-axis of the diagram. Similarly χ represents the Flory-Higgins interaction parameter which reflects the interaction energy between different segments and N represents the degree of polymerization. When the product χN reaches a critical value i.e. $(\chi N)_{ODT}$ (ODT: order-disorder transition), the block copolymer microphase separates into a periodically ordered structure ranging from a length of 5-50 nm.[1,10-12]

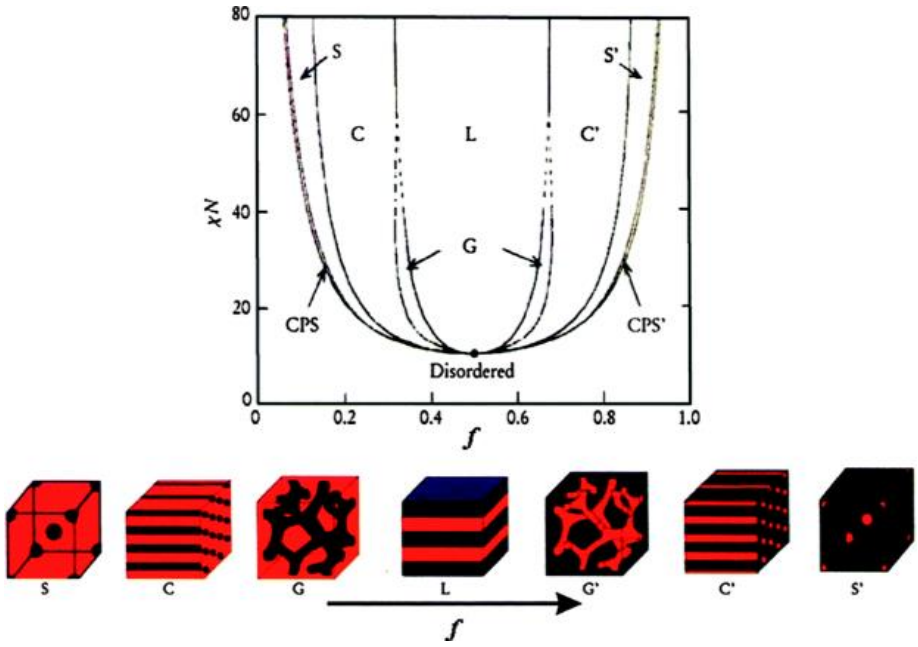

Figure 1.1. The phase diagram of a diblock copolymer. Reproduced with permission from Ref. (10). Copyright 2013 The Royal Society of Chemistry.

As shown in the phase diagram in Figure 1.1, block copolymers have characteristic properties to form a variety of morphology, however morphology is dependent on the volume fraction and the product of Flory-Higgins interaction parameter and degree of polymerization. The diblock copolymer used in this thesis has PEO volume fraction of 0.2 and PS volume fraction of 0.8. Therefore, upon microphase separation and self-assembly, cylindrical morphologies are obtained as explained in the phase diagram.

1.2.2 Fabrication of cylindrical PEO microdomains from PS-*b*-PEO

There are several methods for the fabrication of cylindrical PEO microdomains. Commonly employed methods are spin-coating and solution casting techniques. In the spin-

coating technique, droplets of polymer solution are placed on a spinning solid substrate. Polymer solution is spread onto the substrate due to the rotating motion. However, in this thesis, solution drop-casting method was used for preparing the sandwich polymer films that were used for SMT measurements. During this process, a droplet of polymer solution was placed on a glass substrate and was allowed to flow on the substrate by applying pressure from another small coverslip.[1] Researchers have been using these methods for the fabrication of cylindrical microdomain morphology. For example, Kim and Librera[13] prepared films by solution casting from toluene with polystyrene-polybutadiene-polystyrene (SBS) triblock copolymer. They successfully prepared well-ordered cylindrical polystyrene by using an intermediate evaporation rate (5 nL/s).

Similarly, Russell's group fabricated cylindrical PEO microdomains by spin coating of benzene solution of PS-*b*-PEO on silicon substrates.[14] Thin films prepared by this way gave a rapid and efficient route to fabricate PEO cylinders; however they observed some defects in the film and crystallization of PEO when the sample was stored for a longer time (two months). To solve these issues, Russell's group prepared thin PS-*b*-PEO films on silicon wafers by spin-coating or by solution-casting a benzene solution of the copolymer. They annealed the spin-casted or solution-casted sample for 48 hours in benzene vapors.[15] After solvent annealing, they observed the sample in an atomic force microscope (AFM) and found complete removal of the defects as well as no appearance of the crystallization even after storing the sample for a longer time.

In an another work, Russell's group successfully prepared cylindrical PEO microdomains by blending a homopolymer poly (methyl methacrylate) (PMMA) with PS-*b*-PEO and selectively removing PMMA by exposing the film to UV-light and rinsing with acetic acid.[16] This approach of blending homopolymer with diblock copolymer and finally removing

homopolymer resulted highly oriented and ordered arrays of PEO cylinders. Later on, Li et al also fabricated cylindrical PEO microdomains by blending poly (acrylic acid) (PAA) with PS-*b*-PEO and removing the PAA by dissolving in MilliQ water.[17]

1.2.3 Effect of solvents on the swelling of block copolymer microdomains

The influence of solvents on the morphology of block copolymer microdomains have been investigated extensively over the past several years. In particular, attention has been focused on the role of solvent in the microdomain swelling for the block copolymer system. However, little information has been reported in the literature about the solvent swelling of PS-*b*-PEO systems until now. Research in the PS homopolymer system revealed that solvent present in the polymer film plays a key role in the chain mobility as well as maintaining the film homogeneity.[18] Neutron reflectometry was used to study solvent content in the spin-coated PS homopolymer.[18] In addition; solvent evaporation is another key factor for the microdomain propagation throughout the film thickness.[19]

In the beginning, researchers studied swelling and de-swelling behavior on polystyrene (PS) homopolymer. Buschbaum et al. used in-situ neutron reflectometry to examine swelling and de-swelling of a toluene solution of polystyrene film.[20] In their study, information about film thickness, roughness and solvent penetration were investigated; however, they did not compare the swelling behavior of different solvent systems. In an another work by Wadey et al., a morphological transition from parallel cylinders to hexagonally perforated lamellar to parallel lamellar was observed when solvents of varying solubility parameter is chosen in polystyrene-*block*-polydimethylsilaoxane (PS-*b*-PDMS).[21] They used scanning force microscopy(SFM) and

small-angle X-ray scattering (SAXS) to explain the morphological transition in the PS-*b*-PDMS system. In their work, films were prepared by selecting a range of solvents having different Hansen solubility parameter (HSP), δ, in $MPa^{0.5}$: n-hexane (14.7) to 1,4-dioxane (20.5). Each solvent has specific HSP which represents a combination of dispersion forces, intermolecular force and hydrogen bonds between the molecules.[21,22]

Recently, Karunakaran and coworkers reported that choosing the right PS and PEO block lengths and the right solvent mixture is another key parameter to form ordered nanostructure in block copolymer. In their study, solvent mixtures containing THF/dimethylacetamide (DMAc)/sulfolane showed minimum aggregation resulting in a polymer membrane with regular porous structure.[23] In contrast, polymer solution containing solvent mixtures of DMAc/sulfolane or THF/DMAc did not show porous structures because of the self-aggregation of the copolymer micelles. Therefore, proper solvent systems should be selected to dissolve BCP in order to get expected polymer morphologies.

Nowadays, solvent based approaches including solvent vapor annealing (SVA) and solvent vapor permeation (SVP) as well as shear-based approaches have been widely employed for various BCP systems to get long range aligned PEO microdomains.[24,31] For example, our group performed SVP to form aligned PEO microdomains in a PS-*b*-PEO film sandwiched between two glass plates.[2] Solvent vapor penetrated through the film from the enclosed chamber helps to form aligned microdomains. In that work, three solvent vapor systems (1,4-dioxane, benzene and toluene) were compared to understand the effects of a particular solvent vapor on the microdomain alignments. It was found that 1,4-dioxnae showed 1D trajectories in the vapor penetration direction, indicating the presence of aligned PEO domains. In contrast, the other two solvents showed predominantly 2D trajectories due to a lack of microdomain alignment and

elongation.[2]

It is obvious that we have well-established methods to prepare aligned PEO microdomains. However, lots of work in the PS-*b*-PEO system needs to be done by choosing different solvents like benzene, tetrahydrofuran and methanol while preparing the polymer solution. Most of the reported literature uses benzene as a solvent to dissolve PS-*b*-PEO; however the use of tetrahydrofuran or methanol and their swelling behavior is still unclear. Therefore, it would be useful to compare the swelling behavior of various solvents in PS-*b*-PEO. This thesis aims to explain how solvent plays a role in the swelling of PEO microdomains. Here, SMT is used to characterize the swelling behavior which will be described in the following section.

1.2.4 Single-molecule fluorescence experiment

Single-molecule fluorescence experiments involve the study of individual fluorescent molecules incorporated in the sample, and can provide information that would be hidden in measurements involving a large number of molecules.[25] Techniques for probing single-molecule fluorescence include total internal reflection fluorescence (TIRF) microscopy.[1,2,26] TIRF microscopy helps to reduce the background fluorescence, thereby increasing the signal to noise ratio, which will help to investigate structure and mass transport characteristics of nanostructured materials. Nowadays, single-molecule fluorescence experiments have been widely used for conducting research in the various fields of chemistry, physics and biology. Detection of single molecules by fluorescence excitation was first introduced by Michel Orrit and Jacky Bernard in 1990.[27] Since then, it is becoming an essential tool to carryout research in materials sciences as well as in biological sciences. In order to study the molecular dynamics inside the nanostructured

material either fluorescence correlation spectroscopy (FCS) or single molecule tracking by wide-field microscopy has been used.[28,29] This thesis is focused on the single molecule tracking of the video data recorded on a wide field fluorescence microscope. The detail working mechanism and means of collecting data by wide field fluorescence microscopy is explained in the Experimental section.

1.2.5 Single-molecule tracking (SMT) method

SMT involves observation of the motion of the individual fluorescent dye molecule within a medium. The paths followed by individual molecules in consecutive video frames are linked to form trajectories. In SMT, the trajectories of individual probe molecules give information about probe diffusion coefficients, microdomain radius, microdomain alignments, etc. SMT is becoming a very useful technique for the microscopic study of block copolymer microdomains. In SMT, the simultaneous study of microdomain permeability and dimension is possible.[1,2] However, block copolymer morphologies and microdomain orientations could also be assessed by other conventional methods including small-angle X-ray scattering (SAXS)[29-31] and atomic force microscopy (AFM).[13,30,33] These methods provide average domain structures, spacing and orientations over macroscopic region of the sample. Therefore, microscopic information of block copolymer film can be studied more conveniently by SMT. This thesis uses SMT to evaluate the swelling of PEO microdomains and diffusion coefficient of dye molecules. A demonstration of how trajectories are obtained by linking identical fluorescent spots in different video frames is shown in Figure 1.2.[34]

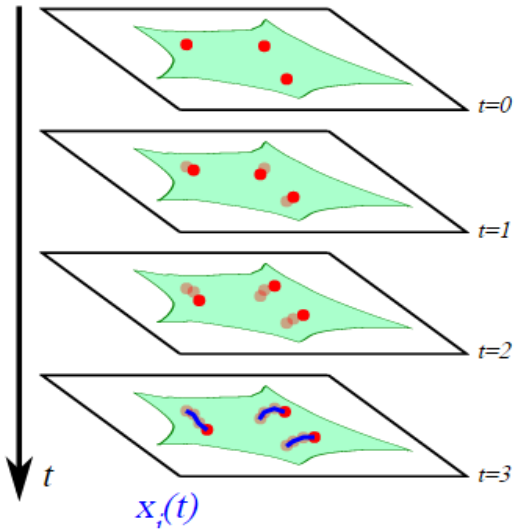

Figure 1.2. A scheme of single molecule tracking: The rectangles represent frames from an image acquisition at times t = 0, 1, 2… The tracked molecules are represented as red circles and in the last frame; the constructed trajectories are shown in blue lines.

Chapter 2 - Experimental Section

2.1 Materials

A block copolymer PS-*b*-PEO (PS, M_n = 35 000 g/mol; PEO, M_n = 10 500 g/mol; PS volume fraction 0.8; M_w/M_n = 1.10) was purchased from Polymer Source and used as received. Benzene (HPLC grade); tetrahydrofuran (HPLC grade); methanol (HPLC grade) and sulforhodamine B (SRB) (ACS grade) were purchased from Acros Organics and used without further purification. A glass coverslip (FisherFinest Premium; 25×25 mm^2, 0.2 mm thick) was employed as a substrate and a thinner glass coverslip (Goldseal cover glass; 22×7 mm^2, 0.1 mm thick) which was cut rectangularly and used as a top piece to make a sandwiched film. Prior to use, both glass pieces were plasma cleaned to remove organic contaminants and kept in a glovebox filled with nitrogen gas. A 20 nM SRB dye stock solution was prepared by dissolving

solid SRB in methanol first and then diluting with benzene. For example: From the stock solution, about 0.8 μL of SRB dye solution is added in the polymer solution in order to obtain a dye concentration of about 5 nM in PEO.

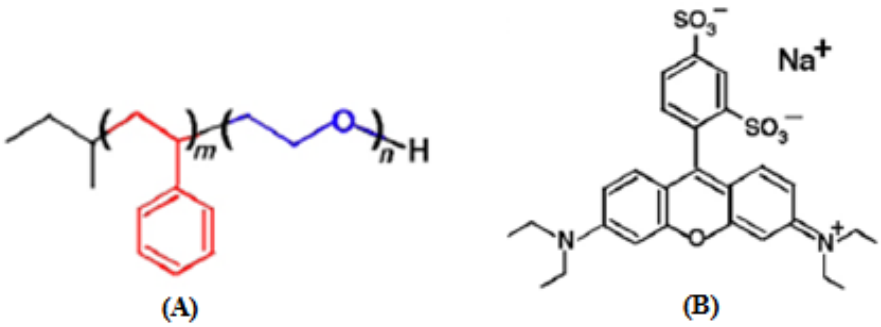

Figure 2.1. Chemical structures of (A) PS-*b*-PEO and (B) Sulforhodamine B (SRB). Reproduced with permission from Ref. (1). Copyright 2014 The American Chemical Society.

2.2 Preparation of PS-*b*-PEO thin films

Dye-doped PS-*b*-PEO sandwiched films for SMT experiments were prepared in a nitrogen-filled glovebox following a procedure previously reported by our group.[1] PS-*b*-PEO was dissolved by using four different solvent systems in order to study swelling behavior for each of them in the PEO microdomains. Benzene, THF, benzene with 14% methanol and THF with 14% methanol were used as solvent which were adjusted to be 25% w/w. During dissolution of polymer, at first a mixture of polymer, solvent and SRB dye solution present in a vial was heated over a hot plate at 45 °C and then stirred in a vortex mixer for a few minutes. After that a droplet of the PS-*b*-PEO solution (50 μL) was placed on a glass coverslip and immediately sandwiched by placing a rectangular shaped glass slide over the droplet. The solution flowed between the two glass plates from one end of the rectangular slide to the other, primarily due to the pressure applied by the top piece. Prior to the SMT experiments, sandwiched films were

dried at 30 °C or 40 °C for 24 hours before the first measurements on a wide field fluorescence microscope were performed. After that, SMT experiments were performed at 24 hour intervals. Experiments were continued for 120 hours (5 days). Samples prepared from benzene solutions (with or without methanol) were dried at 30 °C or 40 °C. Those from THF solutions (with or without methanol) were dried at 30 °C because of its lower boiling point compared with benzene.

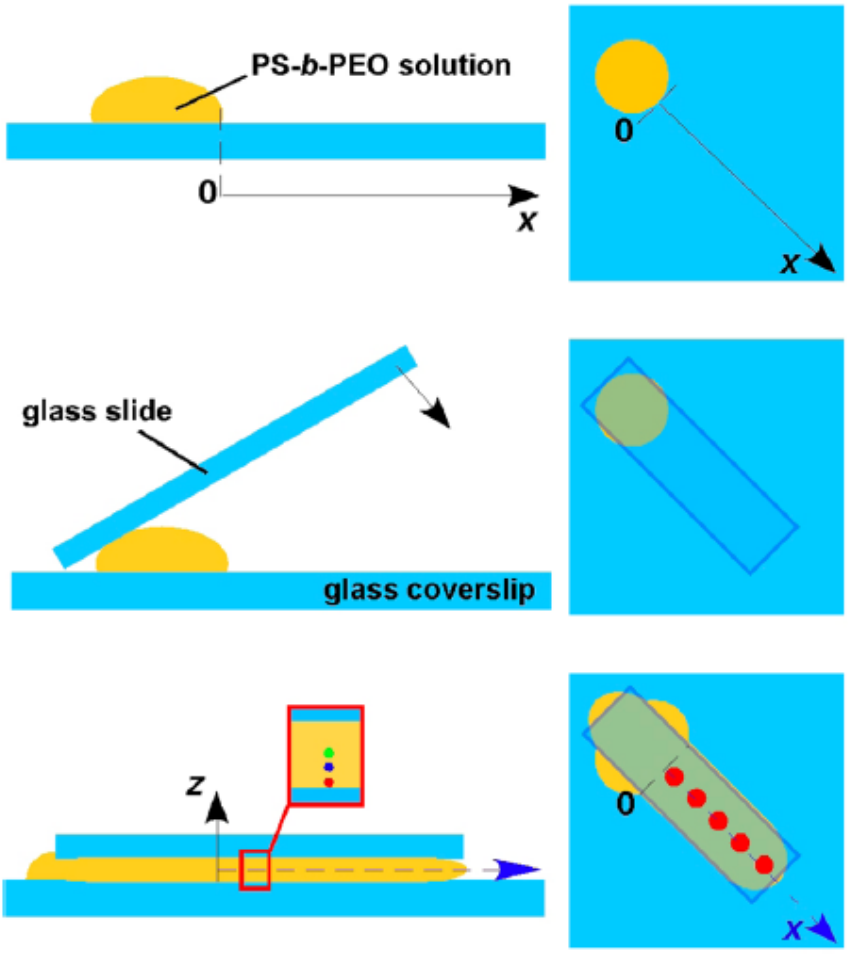

Figure 2.2. Schemes of sample preparation: A droplet (50 µL) of PS-*b*-PEO solution placed on a glass coverslip (top) and immediately sandwiched by a small glass cover slide (rectangular having 8 mm width) to induce pressure driven flow into the solution (middle) and final sandwiched sample (bottom). The film was dried at a constant temperature of 30 °C or 40 °C for

24 hours and SMT data were acquired at five different positions across the sample (shown as red dots; bottom right). Reproduced with permission from Ref. (1). Copyright 2014 The American Chemical Society.

2.3 Instrumentation

2.3.1 Wide-field fluorescence microscopy

Fluorescence images of dye doped PS-*b*-PEO sandwiched films were collected on a wide-field fluorescence microscope. All SMT experiments were performed in a pseudo total internal reflection fluorescence (p-TIRF) mode. In the SMT studies p-TIRF mode was used in order to reduce the background fluorescence from the micrometer-thick polymer film thereby increasing the signal/noise ratio. This system was built on an inverted epi-illumination microscope (Nikon Eclipse Ti) as depicted in Figure 2.3.

Figure 2.3. Nikon Eclipse Ti Microscope

A diagram of the wide field fluorescence microscopy setup is shown in Figure 2.4.[35] Light from a Nd: YVO_4 laser (532 nm) was used for the excitation of single SRB molecules in

the sample. A dichroic beam splitter (Chroma, 555 DCLP) was used to introduce 5 mW laser light into the back aperture of an oil-immersion objective (Nikon Apo TIRF 100X; 1.49NA). The emitted fluorescence was collected by the objective and directed through the dichroic mirror and a bandpass filter (Chroma, 580/40 HQ), before hitting the photosensitive surface of a back-illuminated electron-multiplying CCD camera (Andor iXon DU-897). All SMT videos were 1000 frames in length with frame to frame time of 0.042 second with an electron-multiplying gain of 30, and a readout rate of 10 MHz. The same frame time of 0.042 second was used for the collection of all SMT videos, however molecules move slowly in a sample dried for 5 days. The SMT videos were recorded of 16 × 16 μm^2 film regions as 128 pixels × 128 pixels data (2 × 2 binning;1 pixel = 125 nm). All SMT video data were recorded at five different locations along the flow direction of a sandwiched film near the film- substrate interface ($z \approx 1$ μm). The first measurement was conducted at x = 0 mm from the edge of the initial polymer droplet. Then, other measurements were made of at every 2 mm intervals as a function of distance from the first measurement. SMT measurements were started after 24 hours of drying (30 °C or 40 °C) and measurements were made approximately every 24 hours.

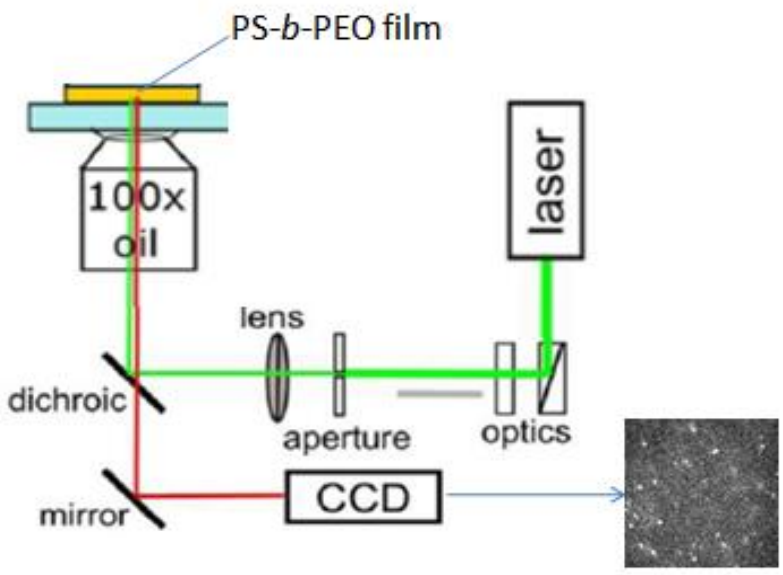

Figure 2.4. Setup for SMT measurements on a wide field fluorescence microscope. Reproduced with permission from Ref. (35). Copyright 2015 The American Chemical Society.

2.4 Analysis of Trajectory data

2.4.1 Spot detection and linking in trajectories

Detection of fluorescent spots present in the video frame and linking into trajectories were done by using ImageJ particle tracker software. Single molecule trajectories were obtained by linking the positions of the individual molecules in consecutive frames. For spot detection purposes, video frames were loaded into the ImageJ software and detection parameters such as the radius, cutoff value and percentile were chosen. Particle radius was chosen based on the size of the spot, which can be estimated by analyzing the spot using the plot profile menu, which gives an approximate radius in pixels. Based on the measured spot size, a suitable radius of 2, 3 or 4 pixels was chosen. The cutoff parameter was chosen to discriminate fluorescent spots and non-fluorescent spots. In our experiment a cutoff value of zero was chosen, assuming that all the bright spots were single molecules. Similarly, the percentile value was chosen to select the brightest candidate spots from the whole video. Small percentile values, for example 0.3 % or 0.4 %, were selected in order to avoid linking errors. However, the chosen percentile should give a sufficient number of trajectories from the detected spots. In general, approximately 10-20 spots should be present for the linking purpose. After spot detection, spot linking was done by selecting appropriate link range and displacement parameters. Link range refers to the number of subsequent frames that are considered for linking. Generally a link range of 1 frame was selected to link spot in subsequent video frames. Similarly, displacement refers to the maximum number of pixels a single molecule is allowed to move between consecutive frames. A displacement of 5

or 6 pixels was chosen to link the fluorescent spots in this project. All these spot detection and linking parameters should be chosen very carefully with visual examination in order to avoid linking errors.

After detecting and linking the spots, all trajectories were plotted for visualization purposes. In this study, single molecule trajectories >10 consecutive frames in length were chosen and the text file obtained was saved and finally analyzed by using Igor Pro software to get 1D, 2D and immobile trajectories.

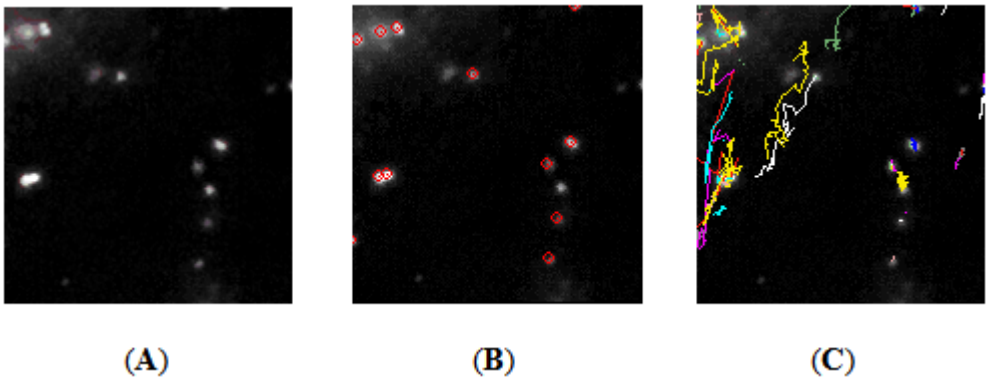

Figure 2.5. Spot detection and linking to form trajectories, A: Video frame used for spot detection, B: Detected spot by Image J plugin, C: Trajectories obtained after linking detected spots. Different colors indicate individual trajectories obtained by linking corresponding spots.

2.4.2 Orthogonal regression analysis of trajectories

Quantitative analysis of individual trajectory segments was performed by using orthogonal linear regression methods[1-3] which involve fitting of individual trajectories to a straight line. A number of parameters, for example in-plane orientation angle, variances of molecular motion along (σ_R^2) and across (σ_δ^2) the trajectory, were obtained as outputs of the regression methods. 1D, 2D and immobile trajectories reflecting 1D-diffusing, 2-D diffusing and

immobile molecules were distinguished based on the variation in single-molecule positions across (σ_δ) and along (σ_R) the trajectories. Specifically, trajectories with σ_δ > 40 nm were classified as 2D , while those with $\sigma_\delta \leq 40$ nm and $\sigma_R \geq 77$ nm were classified as 1D.[1] Trajectories with $\sigma_\delta \leq 40$ nm and $\sigma_R < 77$ nm were identified as immobile.[1] The threshold values for σ_δ and σ_R were estimated from Monte Carlo simulations of single molecule diffusion.[1-3] These simulations employed a signal to noise (S/N) ratio and diffusion coefficient similar to the experimental SMT data.[2,3] SMT gives useful information about 1D, 2D and immobile trajectories, order parameter for 1D trajectories, tilt angles and so on. The present study is primarily focused on 1D trajectories present in each video to estimate microdomain permeability and radius of PS-*b*-PEO films prepared by using solutions of different composition.

2.4.3 Calculation of microdomain radius (*r*), diffusion coefficient (*D*) and tilt angle (θ)

In this work, estimation of the microdomain radius and the diffusion coefficient of the dye molecule inside the PEO domains were undertake to explain the effect of solvent at various drying times. The radius of the PEO microdomains can be obtained from the σ_δ^2 values of 1D trajectories. The measured σ_δ^2 comes from the transverse molecular motion within the microdomains. In addition, position errors obtained from the immobile molecules (σ_{other}^2) from the same video are also necessary to calculate the radius. Microdomain radius was then calculated using the following equation:

$$\sigma_\delta^2 = \sigma_{other}^2 + r^2 \quad \text{..... (1)}$$

For the calculation of diffusion coefficient, the mean square displacement (MSD) as a function of lag time (τ) was first calculated. The relationship used to calculate MSD for 1D diffusing molecules is given by:

$$MSD\ (\tau) = 2D\tau \qquad (2)$$

After getting MSD values, a plot of MSD versus lag time is made and the slope obtained from the plot is used to calculate D.

Similarly, the in-plane orientation angles or tilt angles (θ) provide information about the alignment of cylindrical microdomains found within the films. The tilt angle can be obtained by fitting each 1D trajectory to a straight line relative to the flow direction or solvent vapor penetration (SVP) direction (θ = 0°), which is shown in Figure 2.6:

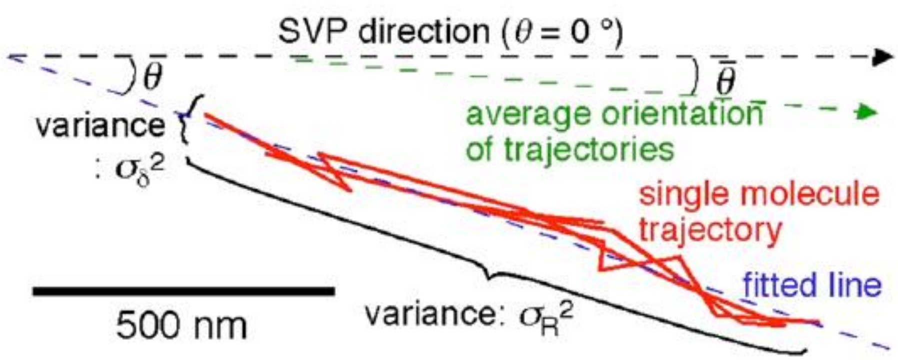

Figure 2.6. A single molecule trajectory (red) fitted to the straight line (blue) in the orthogonal regression method. Reproduced with permission from Ref. (2). Copyright 2012 The American Chemical Society.

Chapter 3 - Results and Discussion

In this study, SMT was used to investigate the solvent swollen PEO microdomains in PS-*b*-PEO films prepared by sandwiching the dye doped polymer solution between two glass plates. The shear based flow of a PS-*b*-PEO solution in benzene or THF between two glass slides is

expected to produce microdomain alignment in the flow direction of the polymer sample.[1] SMT measurements were carried out in the sample after drying the sample at 30 °C (pure benzene, THF) and 40 °C (pure benzene). In addition, two more samples were prepared by using THF with methanol (THF to methanol V/W=50 μl/0.63 mg) and benzene with methanol (benzene to methanol V/W= 50 μl/0.63 mg). These samples were prepared to study the influence of methanol on microdomain swelling. The latter two types of samples were also dried at 30 °C before SMT. In order to discuss the swelling of PEO microdomains, three solvents: benzene, THF and methanol were selected based on the differences in their boiling points and solubility parameters. For example, benzene has a high boiling point (80.1 °C) compared to THF (66 °C) and methanol (64.7 °C). Based on the boiling point values, THF and methanol should evaporate more quickly than benzene from the PS-*b*-PEO films. Similarly, methanol and THF are more polar than benzene which indicates these solvents may preferentially swell the PEO microdomains. In this way, solvents were selected for the swelling of PEO microdomains.

3.1 SMT studies of solvent-swollen microdomains in PS-*b*-PEO films: Pure benzene at 40 °C

In this experiment, SMT data collection was started by using benzene swollen PS-*b*-PEO films dried at 40 °C. SMT videos were collected from the partially dried sandwiched film at 24 hour intervals until 120 hours (5 days) was reached. Five SMT videos were recorded from five different locations in the sample and each video was analyzed by using the orthogonal regression method described in the experimental section. Briefly, SMT videos are loaded into the ImageJ software and spot detection and linking is done to get trajectories, and finally, the data obtained are analyzed by using an Igor macro. A representative wide field video image recorded from the

same sample after 1-5 days of drying and corresponding Z-projection and 1D trajectories from the 1000 frame video is shown in Figure 3.1. These representative SMT videos were recorded at x = 2 mm from the edge of the initial polymer droplet and z = 1 μm from the film- substrate interface.

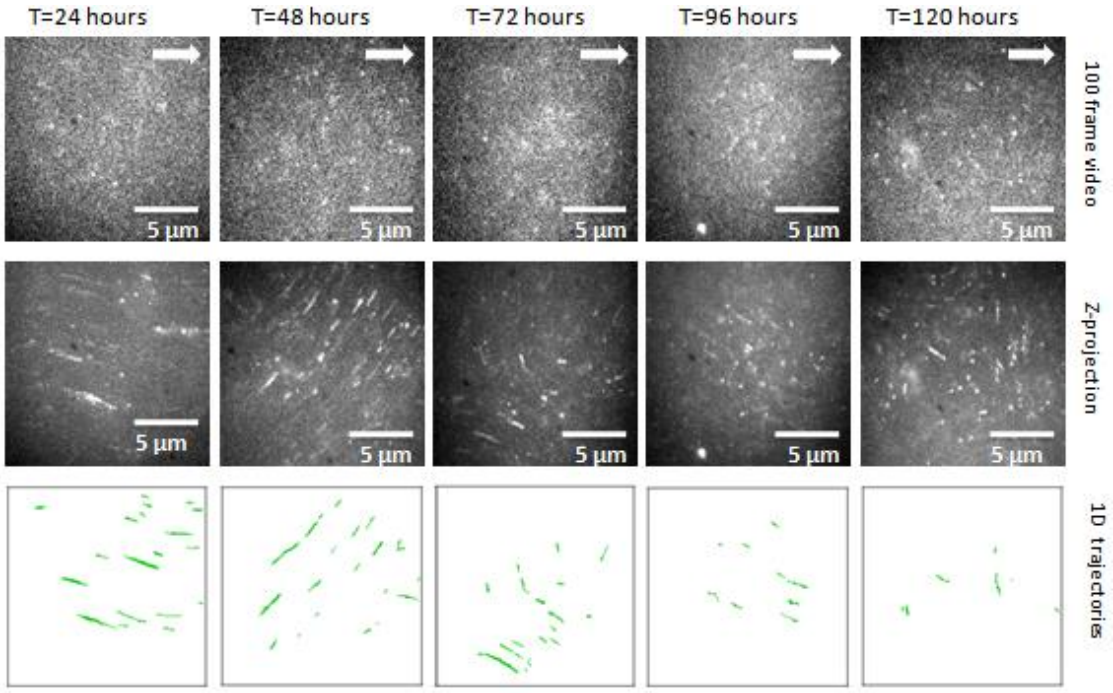

Figure 3.1. Representative SMT video images used for the analysis obtained from the same sample (pure benzene at 40 °C) dried for different times. The arrow in the images shows the flow direction of polymer solution. Below the video images, Z-projection images and 1D trajectories derived from the respective images are shown.

1D trajectories and Z-projection images shown in Figure 3.1 can be used to get information about microdomain alignments. For example the 1D trajectories observed after 24 hours drying are generally found to be better aligned to the solution flow direction than those obtained after 48 hours drying. Alignments of the microdomains vary from one position to another within a sample. This observation suggests the presence of multiple grains in the film. In

addition, the total numbers of 1D trajectories keep decreasing with respect to the drying time. Therefore, only a few 1D trajectories are present after 120 hours (5 days) of drying.

In order to discuss the effect of solvent in the swelling of PEO microdomains, *D* and *r* values were calculated from individual 1D trajectories as a function of drying time (*t*). After that a plot of *D* versus *t* and *r* versus *t* was drawn as shown in Figure 3.2, which represents a collective trend coming from three different samples prepared on different dates, using similar conditions. A gradual decrease in *D* was observed in benzene swollen films even though the difference between one drying point to another is very small (0.1-0.2 $\mu m^2/s$). On the other hand, while looking at the trends of microdomain radius, a sharp decrease of *r* was observed in second day, this indicates that benzene is almost evaporated after 48 hrs of drying.

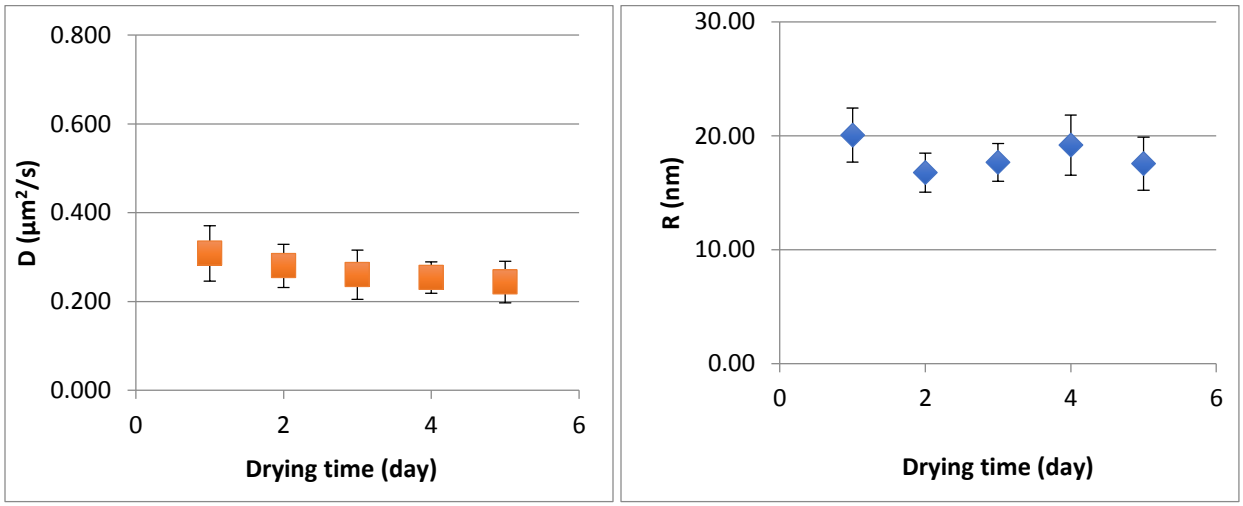

Figure 3.2. Trends in *D* versus *t* (left) and *r* versus *t* (right) for pure benzene at 40 °C

Another important aspect of this work is to get information on the role of different solvents in microdomain alignments. Figure 3.3 depicts the tilt angle distributions obtained from three different samples, prepared on different days following similar sample preparation

conditions. In the Figure 3.3(A) and 3.3(B), the histograms are peaked near θ = 0°, indicating microdomain alignment is in the solution flow direction. However, Figure 3.3(C) showed comparatively poor alignment perhaps due to the presence of multiple grains in the sample. These graphs indiacte that PS-*b*-PEO films prepared from benzene showd heterogenity in the microdomain alignments.

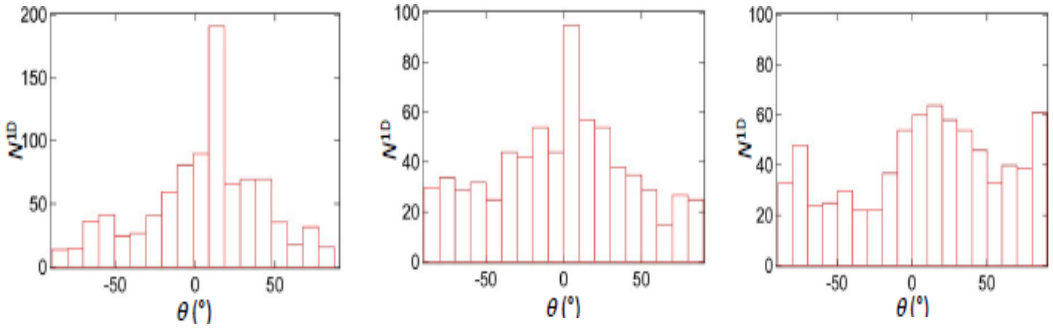

(A) **(B)** **(C)**

Figure 3.3. Histograms showing N^{1D} at different θ obtained from SMT data; A) sample 1, B) sample 2 and C) sample 3.

3.2 SMT studies of solvent-swollen microdomains in PS-*b*-PEO films: Benzene-methanol mixture at 40 °C

To investigate the influence of methanol on the swelling of PEO microdomains, a benzene-methanol mixture was used to dissolve the PS-*b*-PEO. The methods of sample preparation, SMT data collection and SMT data analysis are similar to those used with pure benzene, as explained previously. Representative raw video images, Z-projection images and 1D trajectories obtained from the SMT data analysis are shown in Figure 3.4.

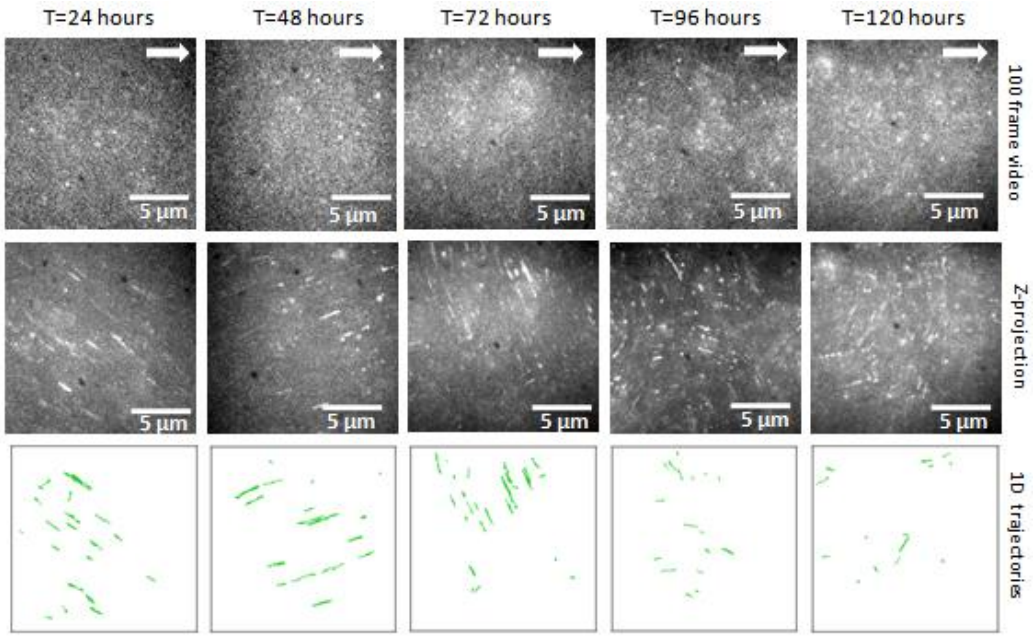

Figure 3.4. Representative SMT video images used for the analysis obtained from benzene-methanol mixture dried for different times. The arrow in the images shows the flow direction of polymer solution. Below the video images, Z-projection images and 1D trajectories derived from the respective images are shown.

As in the benzene-swollen films, films swollen by a benzene-methanol mixture showed larger numbers of 1D trajectories at short drying times. However, the number of trajectories gradually decreased for longer drying times as shown in Figure 3.4. Also, most of the trajectories are tilted, which suggests that the microdomains are not aligned in the solution flow direction.

Similarly, diffusion coefficient and microdomain radius values obtained from individual trajectories were used to obtain the average trend in D and r and thus, to reveal the effects of swelling. These trends (Figure 3.5) are formed by summarizing all data sets recorded from three different samples. The trend in r with respect to t was found to be similar to that of pure benzene which suggests that addition of a small amount of methanol (14% in PEO microdomain) to the

polymer solution composition does not significantly influence microdomain swelling, even though methanol is more polar and thus has a higher preference for PEO.

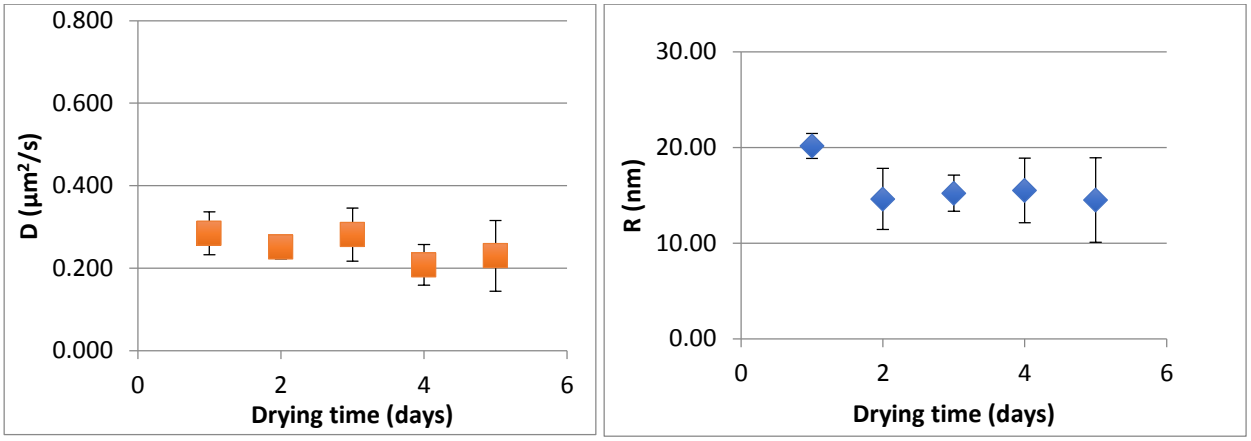

Figure 3.5. Trends in *D* versus *t* (left) and *r* versus *t* (right) for the benzene-methanol mixture.

Histograms of the trajectory tilt angle (θ) of individual 1D trajectories obtained from the SMT data are shown in Figure 3.6 which indicates that microdomain alignments differ from sample to sample. Here, Figure 3.6(B) shows better microdomain alignment compared to Figure 3.6(A). However, if comparison of pure benzene and benzene-methanol mixture is done, no clear conclusion can be drawn because both of the cases show similar levels of alignment.

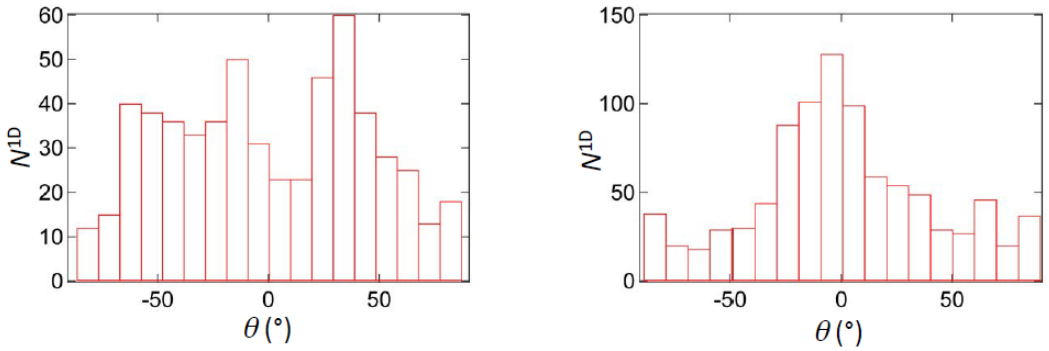

(A) **(B)**

Figure 3.6. Histograms showing N^{1D} at different θ obtained from SMT data; left: sample 1, right: sample 2.

3.3 SMT studies of solvent-swollen microdomains in PS-*b*-PEO films: Pure benzene at 30 °C

In this experiment, SMT data collection was done in benzene swollen films dried at 30 °C. Data obtained from this study will help to compare benzene swollen films dried at 40 °C. When polymer films are dried at higher temperature, solvent present in PEO microdomains may evaporate quickly. Therefore, we can make a direct comparison. The method of sample preparation, data collection and analysis was similar to the SMT studies discussed in the previous section. Representative SMT video images and 1D trajectories obtained from the analysis are shown in Figure 3.7.

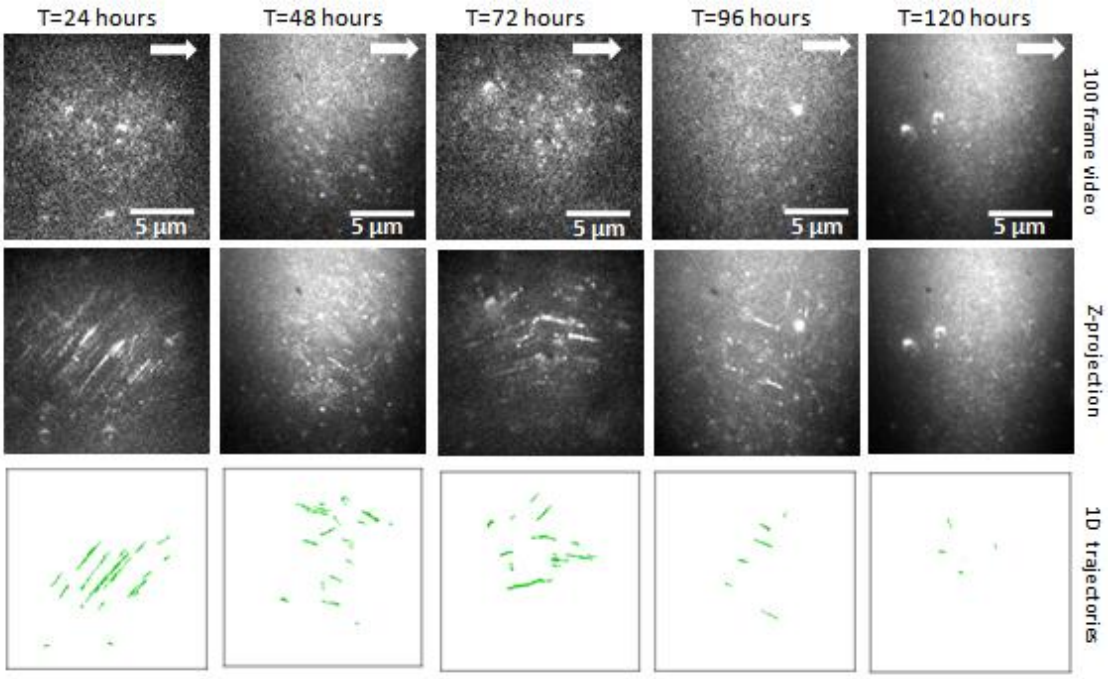

Figure 3.7. Representative SMT video images used for the analysis obtained from the same sample (pure benzene at 30 °C) dried for different times. The arrow in the images shows the flow direction of polymer solution. Below the video images, Z-projection images and 1D trajectories derived from the respective images are shown.

Figure 3.7 shows the number of 1D trajectores decreased as the sample was dried for longer time. This observation was similar in all the solvent systems used for the study. To explain the trend of microdomain swelling, *D* and *r* values obtained from the SMT data analysis which is shown in Figure 3.8.

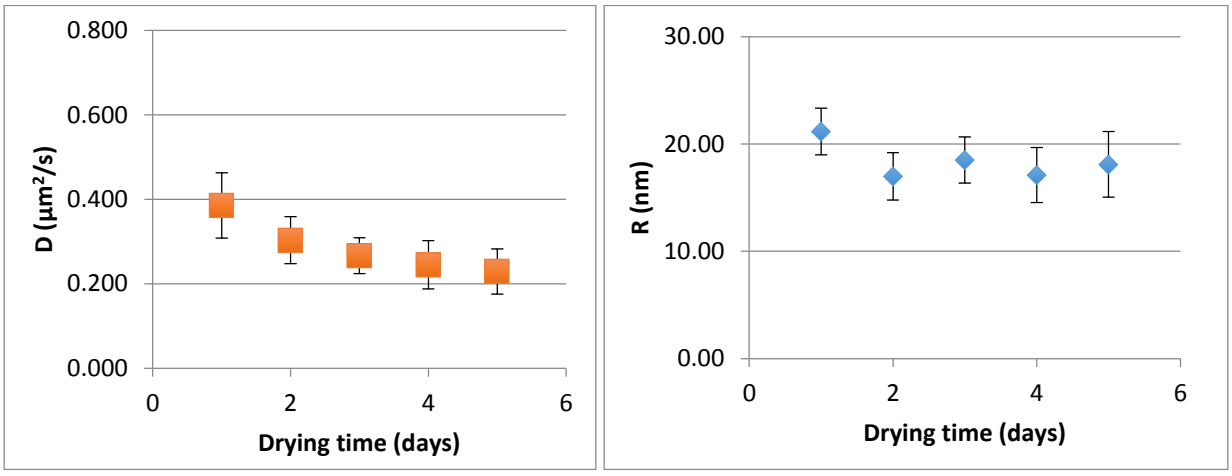

Figure 3.8. Trends in *D* versus *t* (left) and *r* versus *t* (right) for pure benzene at 30 °C

Figure 3.8 shows drying induced trends in *D* and *r* as a function of drying time (*t*). *D* decreased gradually from the first day of drying to the fifth day; however, *r* sharply decreases from the first day to the second but remains nearly constant perhaps due to evaporation of the solvent from the microdomains. Also, a histogram of 1D trajectory tilt angles was drawn (shown in Figure 3.9) to explain the domain alignment.

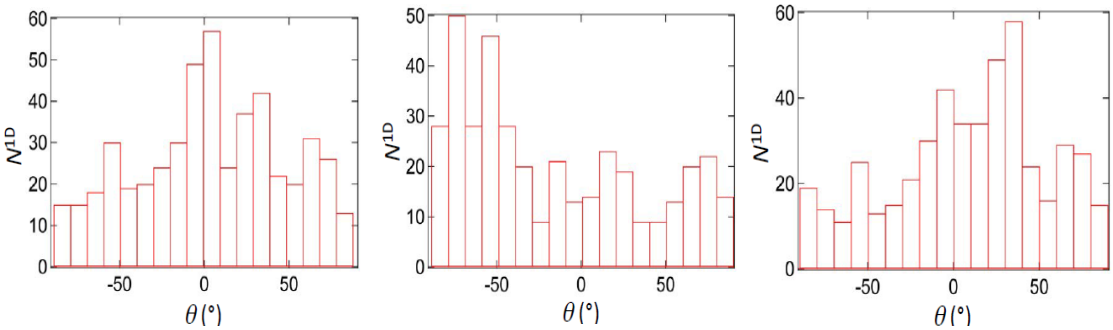

(A) **(B)** **(C)**

Figure 3.9. Histograms showing N^{1D} at different θ obtained from SMT data; A) sample 1, B) sample 2 and C) sample 3.

The histograms shown in Figure 3.9 indicates that sample 1 and 3 has better domain alignment compared to sample 2 because tilt angles are peaked near to $\theta = 0°$, however sample 2 shows heterogeneity in the domain alignment. Therefore, pure benzene did not show perfect domain alignment either at 30 °C or at 40 °C. However, previous studies in our group explained that benzene swollen PS-*b*-PEO film (PS, M_n = 42 000 g/mol; PEO, M_n = 11 500 g/mol) heated at 40 °C produced good microdomain alignments.[1] Better microdomain alignments in that study may be due to the high molecular weight of both the PS and PEO blocks in these studies. In contrast, this study employed smaller PS and PEO (PS, M_n = 35 000 g/mol; PEO, M_n = 10 500 g/mol) polymers which may be responsible for the weaker microdomain alignments.

3.4 Comparison of microdomain swelling: Pure benzene vs benzene-methanol mixture at 40 °C

When comparing the diffusion coefficient and microdomain radius obtained from the both sets of data, similar decreasing trends were observed across all drying times. Also, in both of the cases, *r* decreased significantly from the first day of drying to the second. Similarly, the diffusion coefficient trend in pure benzene showed that *D* decreased gradually across the drying times. However, the benzene-methanol mixture showed some inconsistency. In conclusion, similar trends of *D* and *r* under both sets of conditions suggests that the presence of a small amount of methanol in the polymer solution composition does not have a significant influence on the microdomain swelling even though methanol and benzene have different boiling points and

polymer solubility parameters.

3.5 Comparison of microdomain swelling:

Pure benzene at 30 vs 40 °C

SMT measurements performed in two different samples dried at 30 °C and 40 °C seem to show identical trends in *D* and *r*. However, benzene at 30 °C shows slightly higher *D* and *r* values at initial drying conditions. It is important to note that the average *D* and *r* values appeared to be similar for both conditions, if samples ware dried for a longer time. Therefore, it can be concluded that the trends of diffusion coefficient and microdomain radius remain similar for both drying conditions. The reason behind the higher *D* at 30 °C should reflect the presence of more solvent in the PEO microdomains compared to 40 °C. In contrast, similar trends in microdomain radius for both drying conditions suggest that *r* may be smaller even though *D* is larger and vice versa.

3.6 SMT studies of solvent-swollen microdomains in PS-*b*-PEO films:

Pure THF at 30 °C

In this experiment, THF was chosen as a solvent to investigate its effect on the swelling of PEO microdomains in PS-*b*-PEO films and to compare its swelling behavior with that of benzene. THF is more volatile and has a lower boiling point and has a greater affinity to PEO in comparison to benzene. Therefore, it is interesting to study the effect of THF on microdomain swelling. For this purpose, sandwiched PS-*b*-PEO films were prepared by using THF. PS-*b*-PEO films were dried at 30 °C in a nitrogen filled glovebox and SMT observations were made at 24 hour intervals until 120 hours (5 days). SMT videos obtained from the observation were

analyzed to get 1D trajectories. Representative SMT videos, Z-projection images and 1D trajectories obtained after the analysis are shown in Figure 3.10.

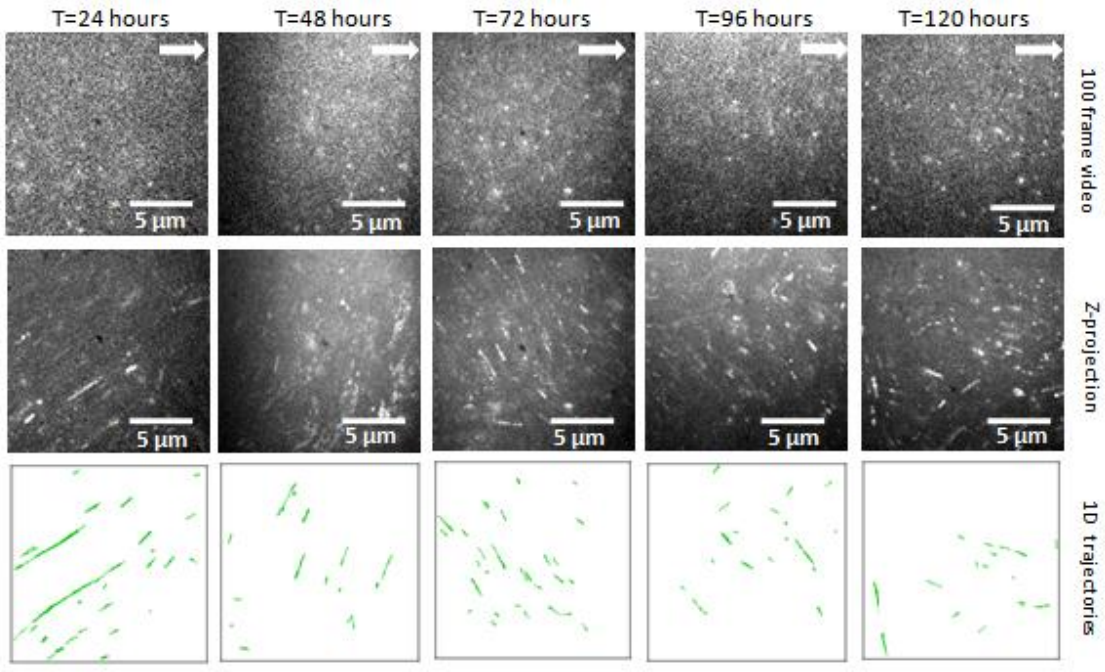

Figure 3.10. Representative SMT video images used for the analysis obtained from the same sample (pure THF at 30 °C) dried for different times. The arrow in the images shows the flow direction of polymer solution. Below the video images, Z-projection images and 1D trajectories derived from the respective images are shown.

SMT videos collected from the sandwiched film were analyzed to get *D* and *r* (from the 1D trajectories) and the average trend of *D* and *r* was obtained by compiling all data collected on different dates. The trends in *D* and *r* as a function of drying time are shown in Figure 3.11.

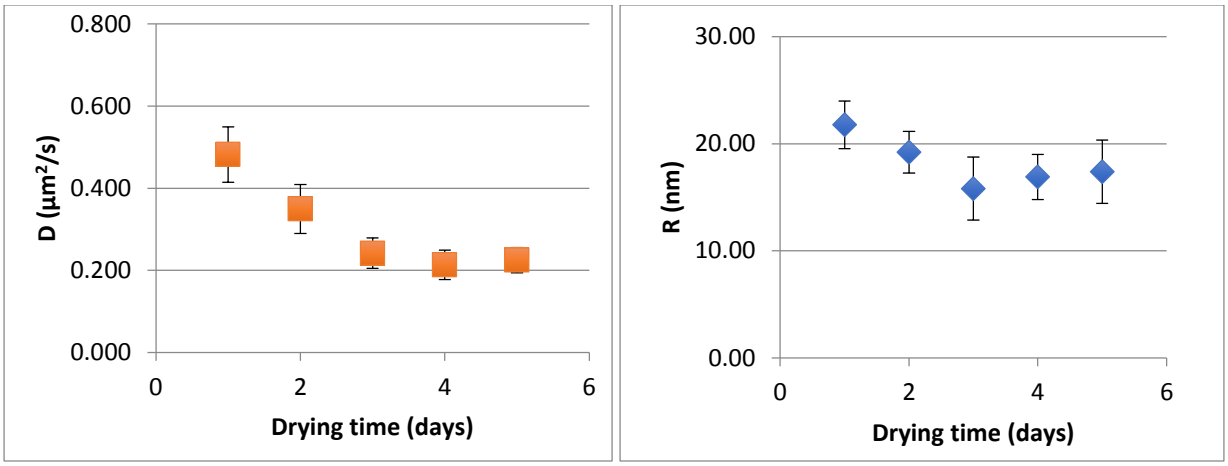

Figure 3.11. Trends in *D* versus *t* (left) and *r* versus *t* (right) for pure THF at 30 °C.

The trends in *D* and *r* as a function of drying time are shown in Figure 3.11, which demonstrates that both *D* and *r* decreased sharply up to the 3rd day. It is interesting to note that *D* and *r* values remain almost constant after the 3rd day, probably because of the almost complete evaporation of THF. Similarly, tilt angle distributions of all 1D trajectories are shown in Figure 3.12 to explain the microdomain alignments. The tilt angle distributions in Figure 3.12(A) is not peaked at θ = 0° indicating poor microdomain alignment in that particular sample, however Figure 3.12(B) and 3.12(C) showed better alignment, which is evident from the distribution of 1D tilt angles near θ = 0°. From these observation, it can be concluded that pure THF also showed heterogeneity in the microdomain alignments.

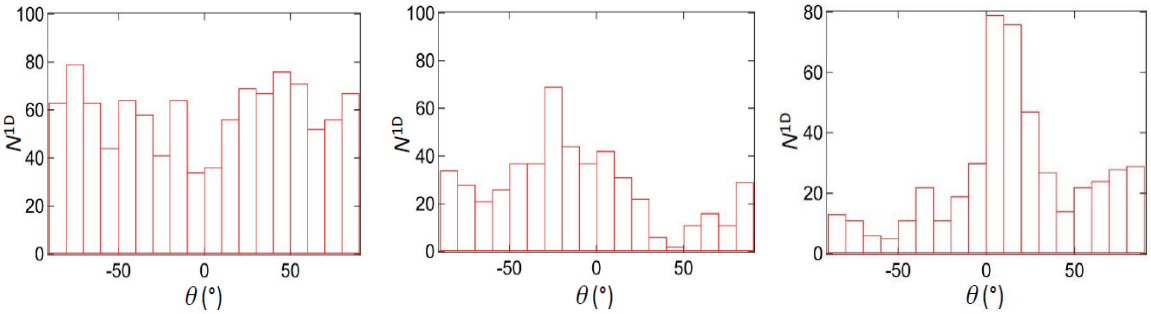

(A) **(B)** **(C)**

Figure 3.12. Histograms showing N^{1D} at different θ obtained from SMT data; A) sample 1, B) sample 2 and C) sample 3.

3.7 SMT studies of solvent-swollen microdomains in PS-*b*-PEO films: THF-methanol mixture at 30 °C

A mixture of THF and methanol was used as a solvent system aiming to study the influence of methanol on microdomain swelling so that a direct comparison can be drawn between films prepared with and without methanol. For this experiment, the method of sample preparation, drying conditions, SMT data collection and data analysis were similar to those used with pure THF. Representative SMT video images, Z-projection images and 1D trajectories obtained after analyzing the SMT data is shown in Figure 3.13. Similar to other solvent systems, the THF-methanol mixture also showed higher *D* and *r* values at the shorter drying times and both *D* and *r* decreased when sample was dried for a longer time.

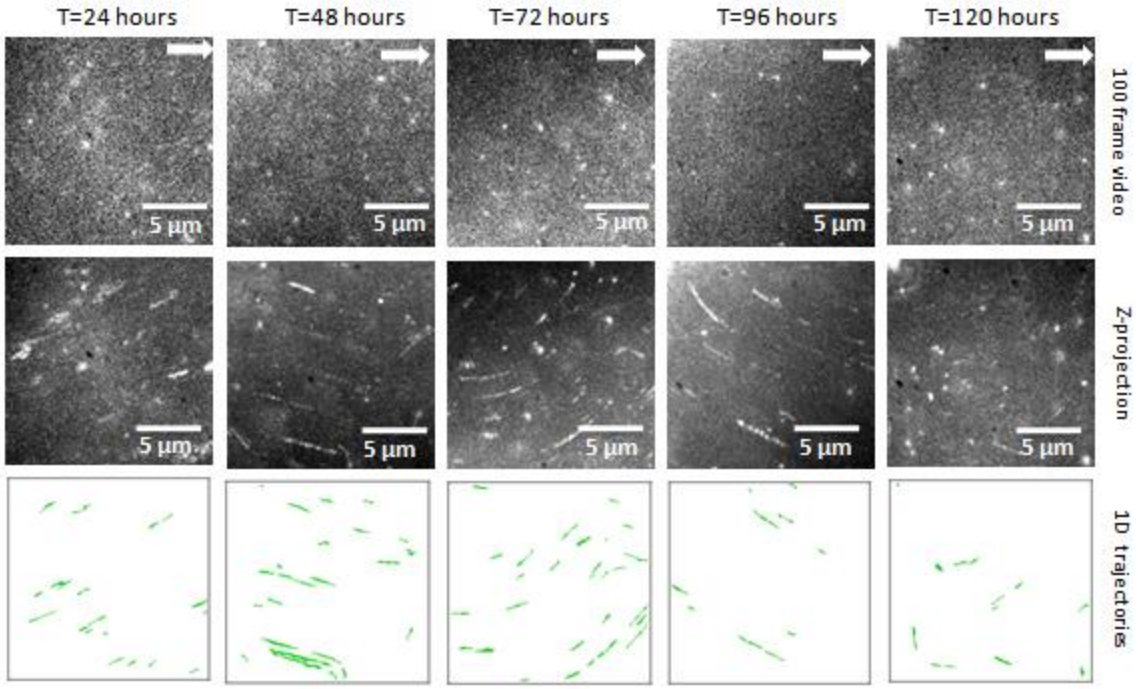

Figure 3.13. Representative SMT video images used for the analysis obtained from the same sample (THF with methanol at 30 °C) dried for different times. The arrow in the images shows the flow direction of polymer solution. Below the video images, Z-projection images and 1D trajectories derived from the respective images are shown.

Figure 3.13 shows representative 1D trajectories (bottom rows) coming from the video images (upper row). The arrangement of 1D trajectories in the figure indicates that PEO domains are not perfectly aligned in the solution flow direction. When the sample was dried for longer time, the number of 1D trajectory decreased significantly. At the same time, an increase in the number of immobile molecules was observed. This kind of observation was similar in all cases for the different solvent systems. Information about microdomain swelling was obtained on the basis of the *D* and *r* values obtained from the 1D trajectories. The trends in *D* and *r* as a function of drying time are presented in Figure 3.14.

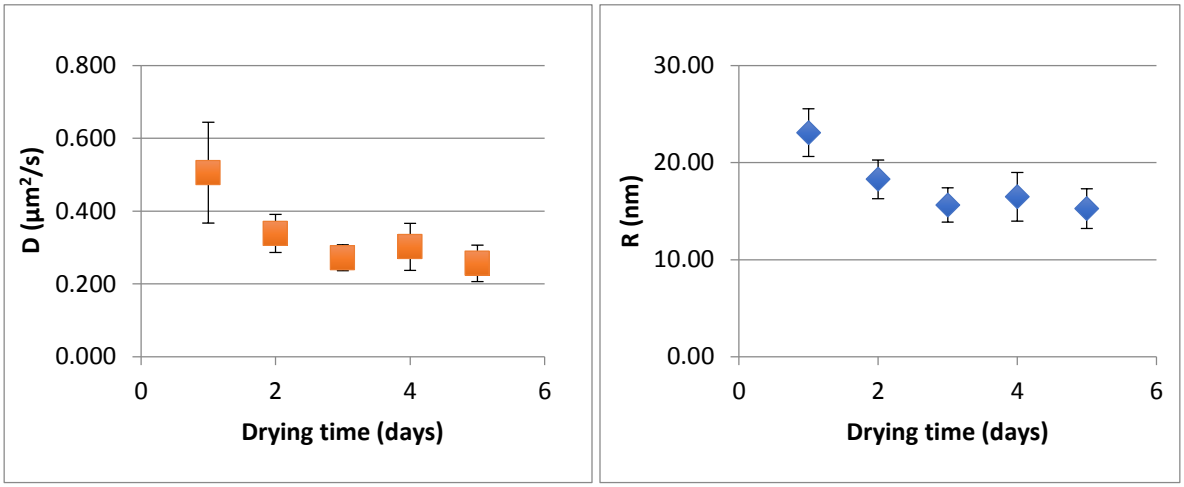

Figure 3.14. Trends in *D* versus *t* (left) and *r* versus *t* (right) for the THF-methanol mixture.

The trends in *D* and *r* from the THF-methanol mixture showed similar trends as a function of drying time (Figure 3.14). The similar trends of diffusion coefficient and radius

indicate that both THF and methanol evaporate from the PEO microdomains across the observed time period. Also, tilt angle distribution (Figure 3.15) was plotted to observe whether methanol plays any role in the microdomain alignments or not.

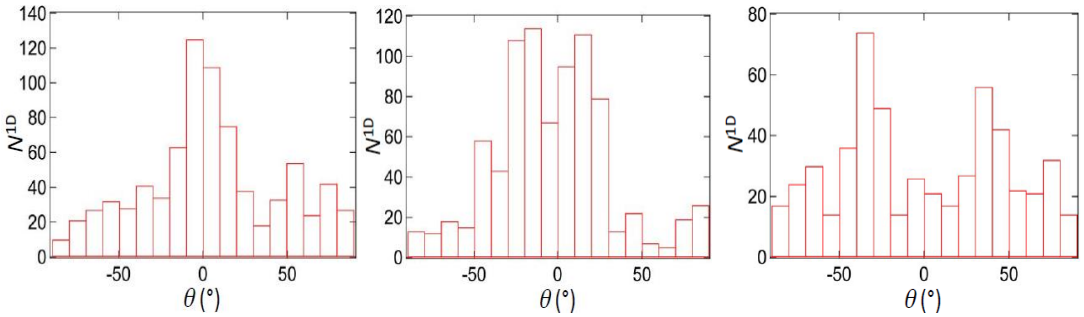

Figure 3.15. Histograms showing N^{1D} at different θ obtained from SMT data; A) sample 1, B) sample 2 and C) sample 3.

Figure 3.15 shows the tilt angle distributions for 3 different samples. Samples 1 and 2 show the best microdomain alignments with their tilt angle distribution near 0°. However, sample 3 shows two Gaussian distributions, indicating multiple grains in the sample. From these observations, it is concluded that addition of methanol in the PS-*b*-PEO does not help to improve domain alignment.

3.8 Comparison of microdomain swelling: Pure THF vs THF-methanol mixture at 30 °C

When data obtained from the pure THF and THF with methanol were compared, they were found to be very similar to each other. Both of the samples exhibited a similar change in *D* and *r*, which is very important observation of this experiment. This data reveals that adding a small amount of methanol to the polymer solution does not help to swell the PEO microdomains.

3.9 Comparison of microdomain swelling: Pure THF vs Pure Benzene at 30 °C

In pure THF, both *D* and *r* sharply decrease up to 3 days of drying, prior to leveling off. The later observation is attributed to evaporation of all THF from the block copolymer microdomains. This observation is in accordance with the low boiling point and high volatility of the THF compared to benzene. In contrast, the sample prepared from pure benzene showed a continuous decreasing trend in *D*, which means that benzene remains in the PEO microdomains longer than THF. However, the *r* value sharply decreases at first and remains almost constant throughout longer drying times.

3.10 Relationship between *D* and *r*

D and *r* values obtained from the analysis of SMT were used to study the relationship between them. For illustration, a graph (Figure 3.16) was plotted which has *D* and *r* values coming from corresponding trajectories (15 trajectories). These 1D trajectory data were obtained from the sample prepared using pure THF. The sandwiched sample was dried for 24 hours before SMT data collection**.** If we look at the individual trajectories and correlate *D* and *r*, trajectories showing high *D* did not consistently show high *r*. Sometimes trajectories having larger *D* gave smaller *r* and vice versa. Observations of the *D* and *r* relationship in benzene and benzene-methanol swollen system also showed similar characteristics. Therefore, we can say that there is no direct correlation between D and *r*.

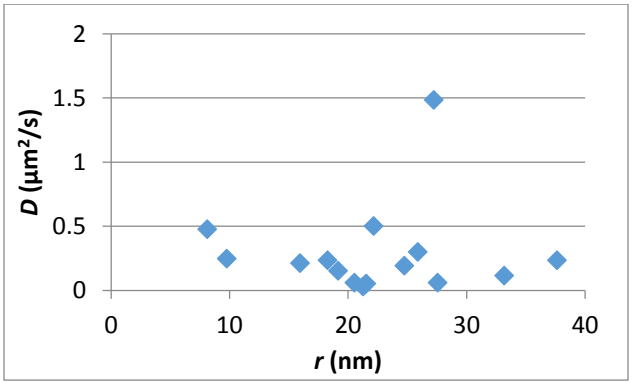

Figure 3.16. A plot of *D* versus *r* values from THF swollen film.

However, if a correlation between *D* and *r* is drawn by using average *D* and *r* values coming from the multiple videos examined under the same conditions, THF and THF-methanol mixture shows a better correlation compared to the benzene and benzene-methanol mixture. Figure 3.17 shows the correlation of *D* and *r* for benzene swollen samples and Figure 3.18 shows the correlation for THF and THF-methanol swollen samples.

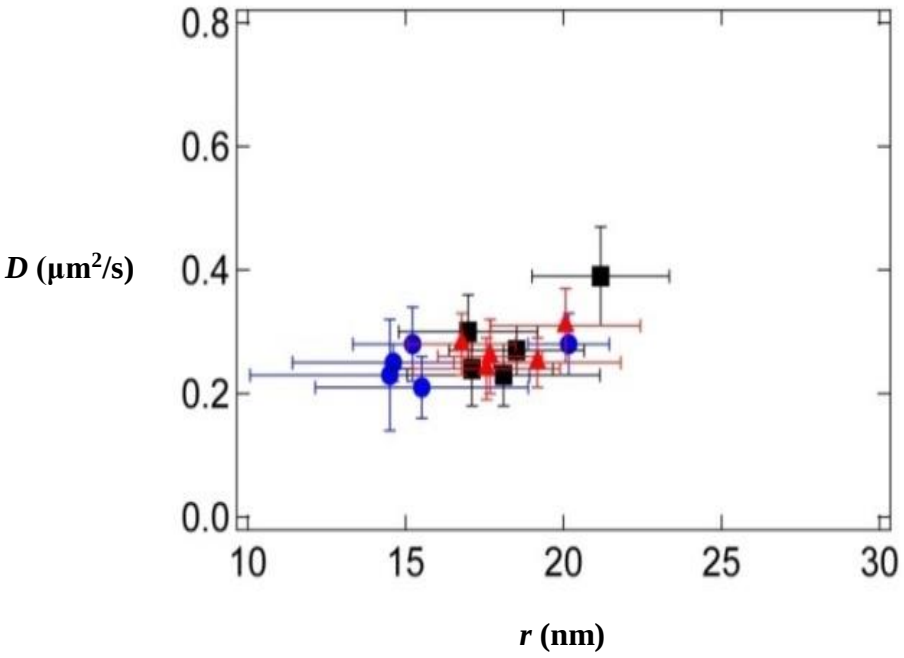

Figure 3.17. Average *D* vs. *r* – Values from benzene and benzene-methanol swollen sample. Black squares: for pure benzene dried at 30 °C, red tringles: pure benzene dried at 40 °C; blue circles: benzene-methanol swollen sample dried at 40 °C.

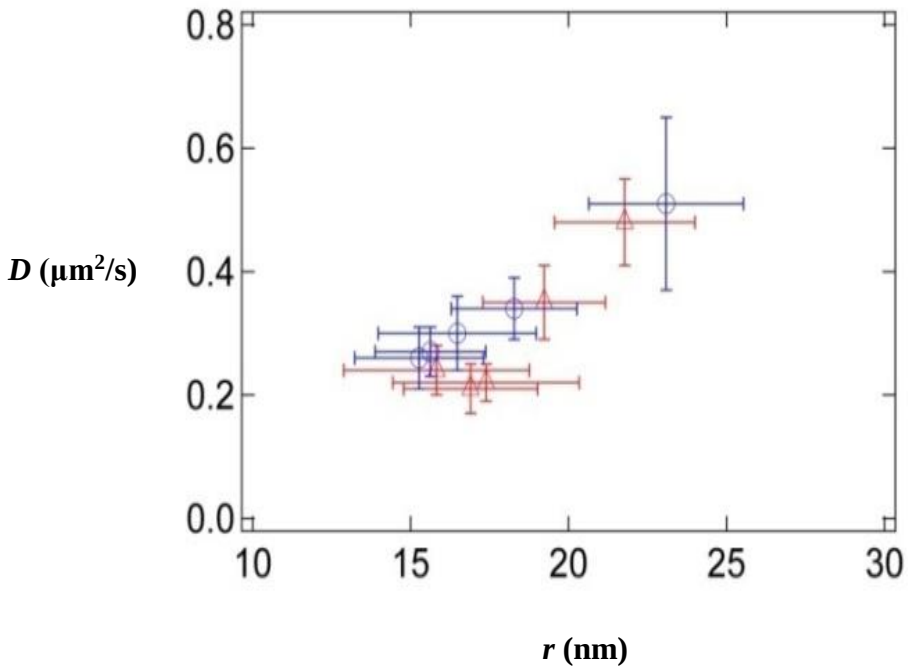

Figure 3.18. *D* vs. *r* – Values from THF and THF-methanol swollen samples.

Red triangles: pure THF dried at 30 °C; blue circles: THF-methanol mixture dried at 30 °C.

Chapter 4 - Conclusions and future directions

This thesis reports the solvent swelling behavior of different solvents present in polymer films. Solvents having different boiling points and solubility parameters were considered. Pure benzene, pure THF, benzene-methanol and THF-methanol mixtures were used to create swelling in the PEO microdomains of the PS-*b*-PEO film. SMT was used to obtain information on the diffusion coefficient, microdomain radius and microdomain alignments. From the data analysis, it was found that both THF and benzene showed similar microdomain swelling behavior at a particular temperature. However, if we compare the data obtained from THF and benzene, a somewhat higher diffusion coefficient for THF swollen films is observed, especially at the initial drying condition (e.g. 1st day). In contrast, both benzene and THF showed similar *D* and *r* values at the longer drying time (e.g. 3rd day). Also, addition of a small amount of methanol to the

solvent mixture does not show any noticeable changes in the swelling and behavior of the PEO microdomains present in the polymer films indicating that methanol is evaporated quickly from the sample. Similarly, the relationship between *D* and *r* was studied for all solvent systems. Correlation of *D* and *r* was done in both experimental data as well as individual videos. There was no clear trend of correlation between *D* and *r*; however THF and THF-methanol mixture showed relatively better correlation compared to benzene and benzene-methanol mixture.

PS-*b*-PEO is currently attracting significant interest in the BCP research community because of its possible application in a variety of fields including making sensing devices, lithographic masks, lithium ion batteries and separation media. However, much of the study needs to be done to explore the swelling behavior by choosing a variety of solvents having a wide range of boiling points and solubility parameters. In addition, studying swelling behavior by choosing different PS and PEO block lengths might be another interesting field of study. These studies will indeed help to create better understanding of the PS-*b*-PEO system.

References

(1) Tran-Ba, K.-H.; Higgins, D. A.; Ito, T. Single-Molecule Tracking Studies of Flow-Induced Microdomain Alignment in Cylinder-Forming polystyrene-Poly(ethylene oxide) Diblock Copolymer Films. *J. Phys. Chem. B* **2014**, *118*, 11406-11415.

(2) Tran-Ba, K.-H.; Finley, J. J.; Higgins, D. A.; Ito, T. Single-Molecule Tracking Studies of Millimeter-Scale Cylindrical Domain Alignment in Polystyrene-Poly(ethylene oxide) Diblock Copolymer Films Induced by Solvent Vapor Penetration. *J. Phys. Chem. Lett.* **2012**, *3*, 1968-1973.

(3) Tran Ba, K. H.; Everett, T. A.; Ito, T.; Higgins, D. A. Trajectory Angle Determination in One Dimensional Single Molecule Tracking Data by Orthogonal Regression Analysis. *Phys. Chem. Chem. Phys.* **2011**, *13*, 1827-1835.

(4) Ito, T. Block Copolymer-Derived Monolithic Polymer Films and Membranes Comprising Self-Organized Cylindrical Nanopores for Chemical Sensing and Separations. *Chem. Asian J.* **2014**, *9*, 2708-2718.

(5) Olson, D.A.; Chen, L.; Hillmyer, M.A. Templating Nanoporous Polymers with Ordered Block Copolymers. *Chem. Mater*. **2008**, *20*, 869-890.

(6) Hillmyer, M.A. Nanoporous Materials from Block Copolymer Precursors. *Adv. Polym. Sci*. **2005**, *190*,137-181.

(7) Jackson, E. A.; Hillmyer, M.A. Nanoporous Membranes Derived from Block Copolymers: From Drug Delivery to Water Filtration. *ACS Nano* **2010**, *52*, 1-16.

(8) Kameta, N.; Minamikawa, H.; Masuda, M. Supramolecular Organic Nanotubes:How to utilize the Inner Nanospace and the Outer Space. *Soft Matter* **2011**, *7*, 4539-4561.

(9) Corma, A. Film Microporous to Mesoporous Molecular Sieve Materials and Their Use in catalysis. *Chem. Rev.* **1997**, *97*, 2373-2419.

(10) Mai, Y.; Zhang, F.; Feng. X. Polymer-Directed Synthesis of Metal-Containing nanomaterials for Electrochemical Energy Storage. *Nanoscale* **2014**,*6*,106.

(11) Mai,Y.; Eisenberg, A. Self-Assembly of Block Copolymer. *Chem.Soc.Rev*. **2012**,*41*,5969-5985.

(12) Orilall, M. C.; Wiesner, U. Block Copolymer Based Composition and Morphology Control in Nanostructured Hybrid Materials for Energy Conversion and Storage: Solar Cells, Batteries, and Fuel Cells. Chem.Soc.Rev. **2011**,*40*,520-535.

(13) Kim, G.; Libera, M. Morphological Development in Solvent-Cast Polystyrene-Polybutadiene-Polystyrene (SBS) Triblock Copolymer Thin Films. *Macromolecules*

1998,*31*,3569-2577.

(14) Lin, Z.;Kim,H.D.;Wu,X.;Boosahda,L.;Stone,D.;Larose,L.,Russell,T.P. A Rapid Route to Arrays of Nanostructures in Thin Films. *Adv Mater* **2002**,*14*,1373-1376.

(15) Kim, S. H.; Misner, J.M.; Xu,T.; Kimura,M.;Russell,T.P. Highly oriented and ordered array from block copolymers via solvent evaporation. *Adv Mater* **2004,** *16*, 226-231.

(16) Kim, S. H.; Misner, J.M.; Russell,T.P. Solvent-Induced Ordering in Thin Film Diblock Copolymer/Homopolymer Mixtures. *Adv Mater* **2004,** *16*, 2119-2123.

(17) Li, X.; Fustin, C.A.; Lefevre,N.; Gohy,J.F.; Feyter,S.D.; Baerdemaeker,J.D.;Eagger,W.; Vakelecom,I.F. Ordered nanoporous membranes based on diblock copolymers with high chemical stability and tunable separation properties. *J.Mater.Chem.*,**2010,** *20*, 4333-4339.

(18) Perlich, J.; Korstgens, V.; Metawalli,E.; Schulz,L.; Georgii,R.; Buschbaum,P.M. Solvent Content in ThIN Spin-Coated Polystyrene Homopolymer Films. *Macromolecul es* **2009,** *42*, 337-344.

(19) Phillip, W.A.; Hillmyer, M.A.; Cussler,E.L. Cylinder Orientation Mechanism in Block Copolymer Thin Films Upon Solvent Evaporation. *Macromolecules* **2010**,*43*,7763-7770.

(20) Buschbaum,P.M.; Bauer, E.; Maurer,E.; Nelson,A.; Cubitt,R. In-Situ Neutron Reflectometry Probing Competitive Sweelling and De-swelling of Thin Polystyrene Films. *Phys. Stat. Sol.*,**2007,** *2*, 68-70.

(21) Wadey, M. L.; Hsieh, I. F.; Cavicchi,K.A.; Stephen,Z.; Cheng, D. Solvent Dependence of The Morphology of Spin-Coated Thin Polydimethylsiloxane-Rich Polystyrene-block-Polydimethylsiloxane Copolymers. *Macromolecules* **2012**, *45*, 5538-5545.

(22) Miller-Chou, B. A.; Koenig, J. L. A Review of Polymer Dissolution. *Prog. Polym. Sci*.**2003**, *28*, 1223-1270.

(23) Karunakaran, M.;Nunes,S.P.; Qiu,X.; Yu,H.; Pienemann, K.V. Isoporous PS-b-PEO Ultrafiltration Membranes via Self-Assembly and Water Induced Phase Separation. *Journal of Membrane Science* **2014,** *453*, 471-477.

(24) Sinturel, C.;Vayer,M.; Morris,M.; Hillmyer, M.A. Solvent Vapor Annealing of Block Polymer Thin Films. *Macromolecules* **2013,** *46* (14),5399-5415.

(25) Ruthardt, N.;Lamb,D.C.; Brauchle,C. Single-Particle Tracking as a Quantitative Microscopy-based Approach to Unravel Cell Entry Mechanisms of Virus and Pharamaceutical Nanoparticles. *Molecular Therapy* **2011,** *7*,1199-1211.

(26) Mattheyses, A.L.; Simon. S.M.; Rappoport. J.Z. Imaging with Total Internal Reflection Fluorescence Microscopy for the Cell Biologist. *Journal of Cell Sci.* **2010,** *123*, 3621-3628.

(27) Orrit, M.; Bernard, J. Single Pentcene Molecules Detected by Fluorescence Excitation in a *p*-terphenyl Crystal. *Phys. Rev. Lett.* **1990**, *65*, 2716-2719.

(28) Ye, F.; Cui, C.; Kirkeminde, A.; Dong, D.; Collinson, M. M.; Higgins, D.A. Fluorescence Spectroscopy Studies of Silica Film Polarity Gradients Prepared by Infusion-Withdrawal Dip-Coating. *Chem. Mater* **2010**, *22*, 2970-2977.

(29) Schmidt, T.; Schutz, G. J.; Baumgartner, W.; Gruber, H. J.; Schindler, H. Imaging of Single Molecule Diffusion. *Biophysics* **1996**, *93*, 2926-2929.

(30) Zhang, M.; Yang, L.; Yurt, S.; Misner, M. J.;Chen, J. T.; Coughlin, E. B.; Venkataraman, D.; Russell, T. P. Highly Ordered Nanoporous Thin Films from Cleavable Polystyrene-block-Poly-(ethylene oxide). *Adv. Mater.* **2007**, *19*, 1571-1576.

(31) Bang, J.; Kim, B. J.; Stein, G. E.; Russelll, T. P.; Li, X.; Wang, J.; Kramer, E J.; Hawker, C. J. Effect of Humidity on the Ordering of PEO-Based Copolymer Thin Films. *Macromolecules* **2007**,*40*,7019-7025.

(32) Osuji, C. O. Alignment of Self-Assembled Structures in Block Copolymers Films by Solvent Vapor Permeation. *Macromolecules* **2010**,*43*,3132-3135.

(33) Albert, J. N. L; Bogart, T. D.; Lewis, R. L.; Beers, K. L.; Fasolka, M. J.; Hutshison, J. B.; Vogt, B. D.; Epps, T. H., III. Gradient Solvent Vapor Annealing of Block Copolymer Thin Films Using Microfludic Mixing Device. *Nano Lett.* **2011**,*11*,1351-1357.

(34) https://en.wikipedia.org/wiki/Single_particle_tracking

(35) Tran-Ba, K.-H.; Higgins, D. A.; Ito, T. Fluorescence Recovery after Photobleaching and Single-Molecule Tracking Measurements of Anisotropic Diffusion within Identical Regions of a Cylinder-Forming Diblock Copolymer Film. *Anal. Chem.* **2015**, *87*, 5802-5809.